Hindawi
Journal of Chemistry
Volume 2017, Article ID 4619159, 13 pages
https://doi.org/10.1155/2017/4619159

Research Article

Characterization, Dissolution, and Solubility of Zn-Substituted Hydroxylapatites $[(Zn_xCa_{1-x})_5(PO_4)_3OH]$ at 25°C

Xin Zhao,[1] Yinian Zhu,[2] Zongqiang Zhu,[3] Yanpeng Liang,[3] Yanlong Niu,[2] and Ju Lin[2]

[1]*College of Light Industry and Food Engineering, Guangxi University, Nanning 530004, China*
[2]*College of Environmental Science and Engineering, Guilin University of Technology, Guilin 541004, China*
[3]*Guangxi Key Laboratory of Environmental Pollution Control Theory and Technology, Guilin University of Technology, Guilin 541004, China*

Correspondence should be addressed to Yinian Zhu; zhuyinian@glut.edu.cn and Zongqiang Zhu; zhuzongqiang@glut.edu.cn

Received 21 March 2017; Revised 2 May 2017; Accepted 10 May 2017; Published 15 June 2017

Academic Editor: Henryk Kozlowski

A series of Zn-substituted hydroxylapatites $[(Zn_xCa_{1-x})_5(PO_4)_3OH$, Zn-Ca-HA] with the Zn/(Zn + Ca) molar ratio (X_{Zn}) of 0~0.16 was prepared and characterized, and then the dissolution of the synthesized solids in aqueous solution was investigated by batch experiment. The results indicated that the aqueous zinc, calcium, and phosphate concentrations greatly depended on the Zn/(Zn + Ca) molar ratio of the Zn-Ca-HA solids (X_{Zn}). For the Zn-Ca-HA dissolution at 25°C with an initial pH of 2.00, the final solution pH increased, while the final solution calcium and phosphate concentrations decreased with the increasing X_{Zn}. The final solution zinc concentrations increased with the increasing X_{Zn} when $X_{Zn} \leq 0.08$ and decreased with the increasing X_{Zn} when X_{Zn} = 0.08~0.16. The mean K_{sp} values for $(Zn_xCa_{1-x})_5(PO_4)_3OH$ at 25°C decreased from $10^{-57.75}$ to $10^{-58.59}$ with the increasing X_{Zn} from 0.00 to 0.08 and then increased from $10^{-58.59}$ to $10^{-56.63}$ with the increasing X_{Zn} from 0.08 to 0.16. This tendency was consistent with the dependency of the lattice parameter *a* on X_{Zn}. The corresponding free energies of formation (ΔG_f^o) increased lineally from −6310.45 kJ/mol to −5979.39 kJ/mol with the increasing X_{Zn} from 0.00 to 0.16.

1. Introduction

Phosphate apatites form an enormous mineral group due to their huge isomorphic capacity [1, 2], which play an important role in many research areas such as biomaterials and environmental science [3–7].

As the main inorganic constituent of bone and dental enamel of vertebrates, calcium hydroxylapatite (HA) has been broadly used in osteoinductive coatings, bone replacement and repair, dental orthopaedics, and so forth [3, 6, 8–11]. The substitution of trace ions in hydroxylapatite can affect not only its lattice parameters *a* and *c*, crystallinity, and morphology, but also its dissolution mechanism and other physicochemical properties [10–12]. Zinc is one of the most important essential trace elements for the growth of humans and its incorporation in Ca-hydroxylapatite can significantly improve the bioactivity of Ca-hydroxylapatite [8–10]. The slow release of zinc substituted in an implant Ca-hydroxylapatite material can also promote bone metabolism and growth around the implant. Thus, the zinc-substituted hydroxylapatite can be a novel biomaterial for bone tissue engineering [10, 13].

Calcium hydroxylapatite (HA) can also be applied to immobilize dangerous metallic compounds in metal-contaminated soils and industrial wastewaters due to its huge ion substitution capacity, which can considerably decrease the mobility and bioavailability of Zn^{2+}, Pb^{2+}, Cd^{2+}, Cu^{2+}, Ni^{2+}, and U^{2+} by transforming these toxic metal ions into some new forms having low solubility and high geochemical stability [1, 5, 14–18]. Heavy metal cations can easily substitute for Ca^{2+} in the hydroxylapatite structure and form zinc-calcium hydroxylapatite (Zn-Ca-HA), lead-calcium hydroxylapatite (Pb-Ca-HA), or cadmium-calcium hydroxylapatite (Cd-Ca-HA) through dissolution-precipitation, ion-exchange, or adsorption process [15]. Therefore, a fundamental knowledge of the apatite physicochemical properties, especially the solubility, stability, and water-mineral interaction, is required to

understand mineral evolution and natural phenomenon or to optimize the industrial processes concerning apatite [5, 19, 20].

However, the thermodynamic data for Zn-substituted hydroxylapatites are now lacking, regardless of the fact that its dissolution and elemental release from solid to aqueous solution exert a great influence on the cycling of zinc, calcium, and phosphate. So far, no experiment on the dissolution and stability of the Zn-substituted hydroxylapatite [$(Zn_xCa_{1-x})_5(PO_4)_3OH$] has been carried out, for which little information has been reported in literatures. Hence, no thermodynamic data can be obtained to assess the bioactivity and bioavailability of an implant Zn-Ca-hydroxylapatite biomaterial or the environmental risk of zinc concerning the Zn-substituted hydroxylapatite. Additionally, the previous data and results about the effects of the Zn substitution for the Ca sites on the apatite structure and properties are still ambiguous and rather inconsistent [8–11, 21, 22].

In this work, calcium hydroxylapatite [$Ca_5(PO_4)_3OH$, Ca-HA] and Zn-substituted hydroxylapatites [$(Zn_xCa_{1-x})_5(PO_4)_3OH$, Zn-Ca-HA] with various Zn/(Zn + Ca) atomic ratios were prepared and the influences of zinc replacement on the hydroxylapatite properties were investigated with XRD, FT-IR, FE-SEM, and FE-TEM instruments. Then, the dissolution of the synthesized solids and the release of components (Zn^{2+}, Ca^{2+}, and PO_4^{3-}) were studied, and the solubility product (K_{sp}) and the corresponding free energy of formation (ΔG_f^o) of the Zn-Ca hydroxylapatites were determined.

2. Experimental Methods

2.1. Solid Preparation and Characterization

2.1.1. Synthesis. The synthesis of the Ca-HA and Zn-Ca-HA solids was carried out by the precipitation method after the following precipitation reaction: $5M^{2+} + 3PO_4^{3-} + OH^- = M_5(PO_4)_3OH$, where M = Ca for Ca-HA and (Zn + Ca) for Zn-Ca-HA. An aqueous solution with [P] = 0.12 mol/L was first prepared by dissolving $NH_4H_2PO_4$ into ultrapure water, and a series of the mixed aqueous solutions with [Zn + Ca] = 0.4 mol/L were then prepared by dissolving $Zn(CH_3COO)_2 \cdot 2H_2O$ and $Ca(CH_3COO)_2 \cdot H_2O$ into ultrapure water. The moles of $Zn(CH_3COO)_2 \cdot 2H_2O$ and $Ca(CH_3COO)_2 \cdot H_2O$ were varied in each preparation to get the mixed aqueous solutions with different [Zn]/[Zn + Ca] molar ratios of 0, 0.02, 0.04, 0.06, 0.08, 0.10, 0.12, 0.14, 0.16, 0.18, and 0.20. 250 mL of the Zn^{2+} and Ca^{2+} mixture solution was added to 250 mL of 4.4 mol/L CH_3COONH_4 buffer solution and then 500 mL of the $NH_4H_2PO_4$ solution was also added with vigorous stirring at 23 ± 1°C, which resulted in the forming of white suspension (Table 1). The NH_4OH solution was used to adjust the pH of the resulting suspension to 7.5. The suspension was aged at 100°C for 48 h and then subjected to suction filtration. Finally, the white precipitates obtained were cleaned cautiously with ultrapure water and dried at 70°C for 16 h.

2.1.2. Characterization. 10 mg of each synthetic solid was digested in 20 mL of 1 mol/L HNO_3 solution and then diluted to 100 mL with ultrapure water. It was measured for zinc, calcium, and phosphate using an inductively coupled plasma-optical emission spectrometer (ICP-OES, Perkin-Elmer Optima 7000 DV) to calculate the solid compositions. The solids were measured using a powder X-ray diffractometer (XRD, X'Pert PRO) that was set to 40 kV and 40 mA with a Cu Kα radiation at a scan speed of 0.2°/min. Phase identifications were made by comparing the recorded XRD patterns of the solids with the reference code 00-024-0033 for calcium hydroxylapatite and the reference code 00-020-1427 for ammonium zinc phosphate (NH_4ZnPO_4) from the ICDD standards. A field emission scanning electron microscope (Hitachi FE-SEM S-4800) was used to observe the morphology of each solid.

2.2. Dissolution Experiments. Each dissolution was designed by adding 2.0 g of the synthesized Ca-HA or Zn-Ca-HA to 100 mL of HNO_3 solution (pH = 2) or ultrapure water (pH = 5.6) or NaOH solution (pH = 9) in a series of 150 mL polypropylene bottles, which were then capped and soaked in the water bath of 25°C. From the bottles, 5 mL of the aqueous solutions was sampled at 23 intervals (1, 3, 6, 12, 24, 48, 72, 120, 240, 480, 720, 1080, 1440, 1800, 2160, 2880, 3600, 4320, 5040, 5760, 7200, 7920, and 8640 hours), filtered through a 0.22-μm-pore-size filter and stabilized using 0.2% HNO_3 solution. After each sampling, 5 mL of the corresponding HNO_3 solution, ultrapure water, or NaOH solution was added. The dissolved zinc, calcium, and phosphate in the aqueous solutions were measured using ICP-OES. After 8640 h dissolution, the solids were sampled, cleaned, dried, and then examined using XRD, FT-IR, FE-SEM, and FE-TEM.

2.3. Thermodynamic Calculations. The PHREEQC program (version 3) [23] was used to calculate the aqueous activities of Zn^{2+}, Ca^{2+}, PO_4^{3-}, and OH^-, and then the ion activity product (IAP) for Ca-HA and Zn-Ca-HA was determined after the mass-action expression. The minteq.v4.dat and llnl.dat databases were chosen in the simulation [24]. The following solution species were considered in the calculation: Zn^{2+}, $ZnOH^+$, $Zn(OH)_2^0$, $Zn(OH)_3^-$, $Zn(OH)_4^{2-}$, $ZnPO_4^-$, $ZnHPO_4$, and $ZnH_2PO_4^+$ for zinc; Ca^{2+}, $CaOH^+$, $CaPO_4^-$, $CaHPO_4$, and $CaH_2PO_4^+$ for calcium; and PO_4^{3-}, HPO_4^{2-}, $H_2PO_4^-$, $H_3PO_4^0$, $CaPO_4^-$, $CaHPO_4$, and $CaH_2PO_4^+$ for phosphate.

3. Results and Discussion

3.1. Solid Characterizations

3.1.1. Chemical Component. The component of the precipitate was dependent on the [Zn]/[Zn + Ca] molar fraction in the starting solution (Table 1). The Zn/(Zn + Ca) molar ratio (X_{Zn}) and the (Zn + Ca)/P molar ratio of each solid sample were equal to the designed composition of the Zn-Ca hydroxylapatites [$(Zn_xCa_{1-x})_5(PO_4)_3OH$] when $X_{Zn} \leq 0.16$.

3.1.2. XRD. The XRD results proved that Ca-HA and Zn-Ca-HA before dissolution (Figure 1(a)) and after dissolution

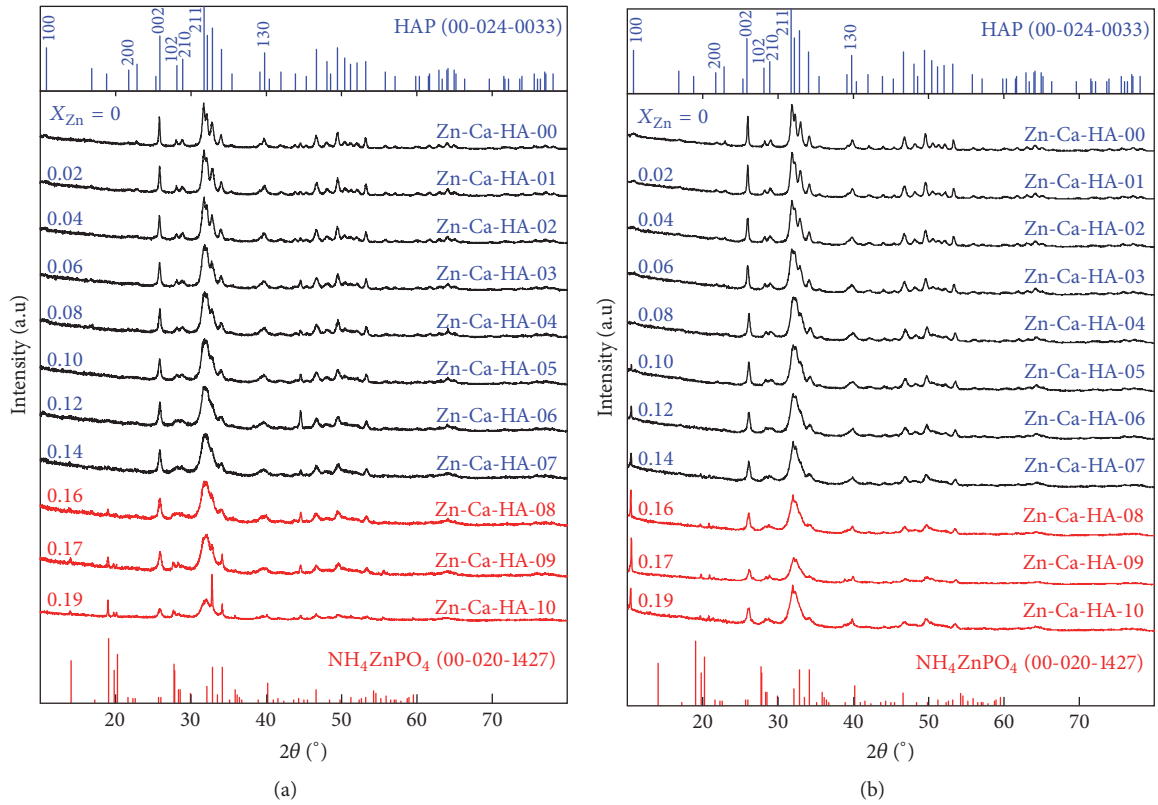

FIGURE 1: X-ray diffractograms (XRD) of the Zn-substituted hydroxylapatites [$(Zn_xCa_{1-x})_5(PO_4)_3OH$] before dissolution (a) and after dissolution at 25°C with an initial pH of 2.00 for 360 d (b).

TABLE 1: Summary of synthesis and composition of the Zn-substituted hydroxylapatites.

Sample number	Volumes of the precursors (mL)				Solid composition
	0.4 M $Zn(CH_3COO)_2{\cdot}2H_2O$	0.4 M $Ca(CH_3COO)_2{\cdot}H_2O$	4.4 M CH_3COONH_4	0.12 M $NH_4H_2PO_4$	
Zn-Ca-HA-00	0	250	250	500	$(Zn_{0.00}Ca_{1.00})_5(PO_4)_3OH$
Zn-Ca-HA-01	5	245	250	500	$(Zn_{0.02}Ca_{0.98})_5(PO_4)_3OH$
Zn-Ca-HA-02	10	240	250	500	$(Zn_{0.04}Ca_{0.96})_5(PO_4)_3OH$
Zn-Ca-HA-03	15	235	250	500	$(Zn_{0.06}Ca_{0.94})_5(PO_4)_3OH$
Zn-Ca-HA-04	20	230	250	500	$(Zn_{0.08}Ca_{0.92})_5(PO_4)_3OH$
Zn-Ca-HA-05	25	225	250	500	$(Zn_{0.10}Ca_{0.90})_5(PO_4)_3OH$
Zn-Ca-HA-06	30	220	250	500	$(Zn_{0.12}Ca_{0.88})_5(PO_4)_3OH$
Zn-Ca-HA-07	35	215	250	500	$(Zn_{0.14}Ca_{0.86})_5(PO_4)_3OH$
Zn-Ca-HA-08	40	210	250	500	$(Zn_{0.16}Ca_{0.84})_5(PO_4)_3OH^*$
Zn-Ca-HA-09	45	205	250	500	$(Zn_{0.17}Ca_{0.83})_5(PO_4)_3OH^*$
Zn-Ca-HA-10	50	200	250	500	$(Zn_{0.19}Ca_{0.81})_5(PO_4)_3OH^*$

*With the forming of ammonium zinc phosphate (NH_4ZnPO_4).

(Figure 1(b)) were the apatite group minerals that belong to the hexagonal crystal system $P6_3/m$. The precipitate of X_{Zn} = 0 was identified to be Ca-HA (ICDD reference code 00-024-0033). The XRD patterns of the Zn-Ca-HA precipitates of $X_{Zn} \leq 0.16$ differed from each other only in their peak location, peak intensity, and peak width. The (002), (211), (102), and (210) reflection peaks of the solid samples shift regularly and slightly to the high-angle direction with the increasing X_{Zn} due to the replacement of Ca^{2+} (0.099 nm) by Zn^{2+} (0.074 nm), which indicated that the Zn-Ca-HA solids were a continuous solid solution when $X_{Zn} \leq 0.16$ [25]. When $X_{Zn} > 0.16$, the characteristic diffraction peaks for ammonium zinc phosphate (NH_4ZnPO_4) were also observed and the peaks for Zn-Ca-HA weakened, which showed that

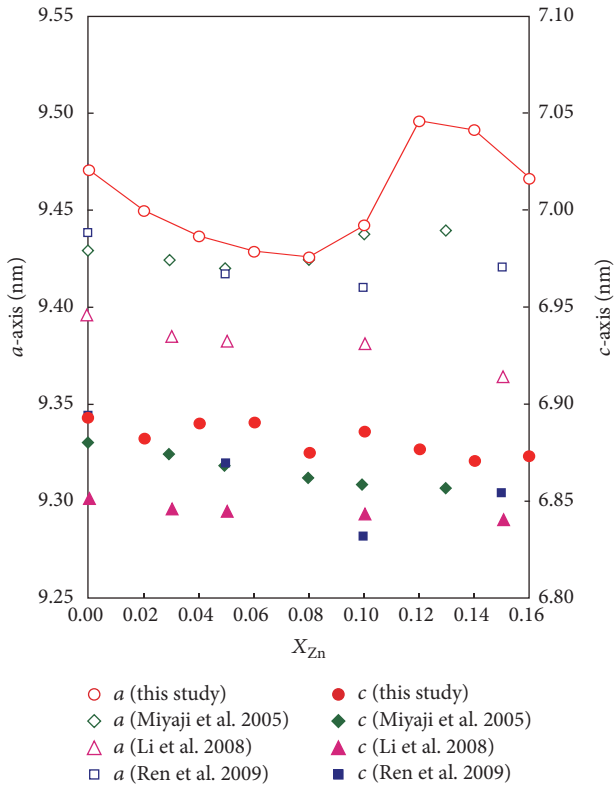

Figure 2: Change of the cell parameters a and c with the increasing X_{Zn} for the Zn-substituted hydroxylapatites $[(Zn_xCa_{1-x})_5(PO_4)_3OH]$.

NH_4ZnPO_4 gradually became the main product; when $X_{Zn} > 0.20$, the diffraction peaks of HA disappeared in our preliminary experiment. The XRD examination showed that the characters of the Ca-HA and Zn-Ca-HA samples before and after dissolution were not obviously distinguishable (Figure 1). No secondary solid phases formed in the Ca-HA and Zn-Ca-HA dissolution.

The continuous Zn-Ca-HA solid solution could be formed within limited X_{Zn} [8, 10, 25]. The solids prepared can be examined for their compositional homogeneity by considering the broadening of the powder XRD peaks of the major reflections [26]. The XRD peak width significantly increased with the increasing X_{Zn} from 0.00 to 0.16, which indicated that the crystallinity of Zn-Ca-HA considerably decreased with the increasing X_{Zn}. On the other hand, the NH_4ZnPO_4 phase formed when $X_{Zn} > 0.16$. The peak intensity of NH_4ZnPO_4 increased and the peak intensity of apatite decreased with the increasing X_{Zn} from 0.16 to 0.20. No parascholzite ($CaZn_2(PO_4)_2{\cdot}2H_2O$) phase was observed when $X_{Zn} = 0.16{\sim}0.20$ [27].

The cell parameter a decreased with the increasing X_{Zn} from 0.00 to 0.08, increased with the increasing X_{Zn} from 0.08 to 0.12, and then decreased with the increasing X_{Zn} from 0.12 to 0.16 (Figure 2), which had also been confirmed by some previous researchers [8, 10, 25]. The cell parameter a decreased up to $X_{Zn} = 0.05$ and began to increase over $X_{Zn} = 0.05$ [25]. The cell parameter a decreased with the increasing X_{Zn} up to 0.10 and increased over $X_{Zn} = 0.10$ [8, 10]. The cell parameter a decreased with a lower zinc substitution in the Ca-HA lattice ($X_{Zn} = 0.00{\sim}0.08$) because the ion radius of Ca^{2+} (0.099 nm) is larger than that of Zn^{2+} (0.074 nm). The increase in the cell parameter a for higher X_{Zn} (0.08~0.12) was attributed to the increasing amount of lattice H_2O that could incorporate in OH sites in the apatite structure [25].

3.1.3. FE-SEM. Figure 3 shows the FE-SEM images of the solids with various $X_{Zn} = 0.00$ to 0.19. The Ca-HA solid ($X_{Zn} = 0.00$) was an aggregate of fine rod-like particles with 20~50 nm in width and 100~150 nm in length. The apatite particle size decreased with the increasing X_{Zn} up to 0.19, which also indicated that the crystallinity of the apatite solids decreased with the increasing X_{Zn}, as showed also in the XRD diffraction (Figure 1).

3.2. Dissolution

3.2.1. Change of Solution pH and Elemental Concentrations with Time. Evolution trends of the solution pH and concentrations of Zn^{2+}, Ca^{2+}, and PO_4^{3-} with time for the Zn-Ca-HA dissolution in HNO_3 solution (pH = 2.00) or ultrapure water (pH = 5.60) or NaOH solution (pH = 9.00) were showed in Figures 4(a), 4(b), and 4(c).

For the Zn-Ca-HA dissolution at 25°C with an initial pH of 2.00 (Figure 4(a)), the solution pH increased from 2.00 to 4.42~4.90 in 1 h dissolution and became stable (pH = 4.88~6.43) after 5040~5760 h dissolution. Commonly, the solution pH increased with the increasing Zn/(Zn + Ca) molar ratios of the Zn-Ca apatites (X_{Zn}) (Figure 5). The solution Zn^{2+},

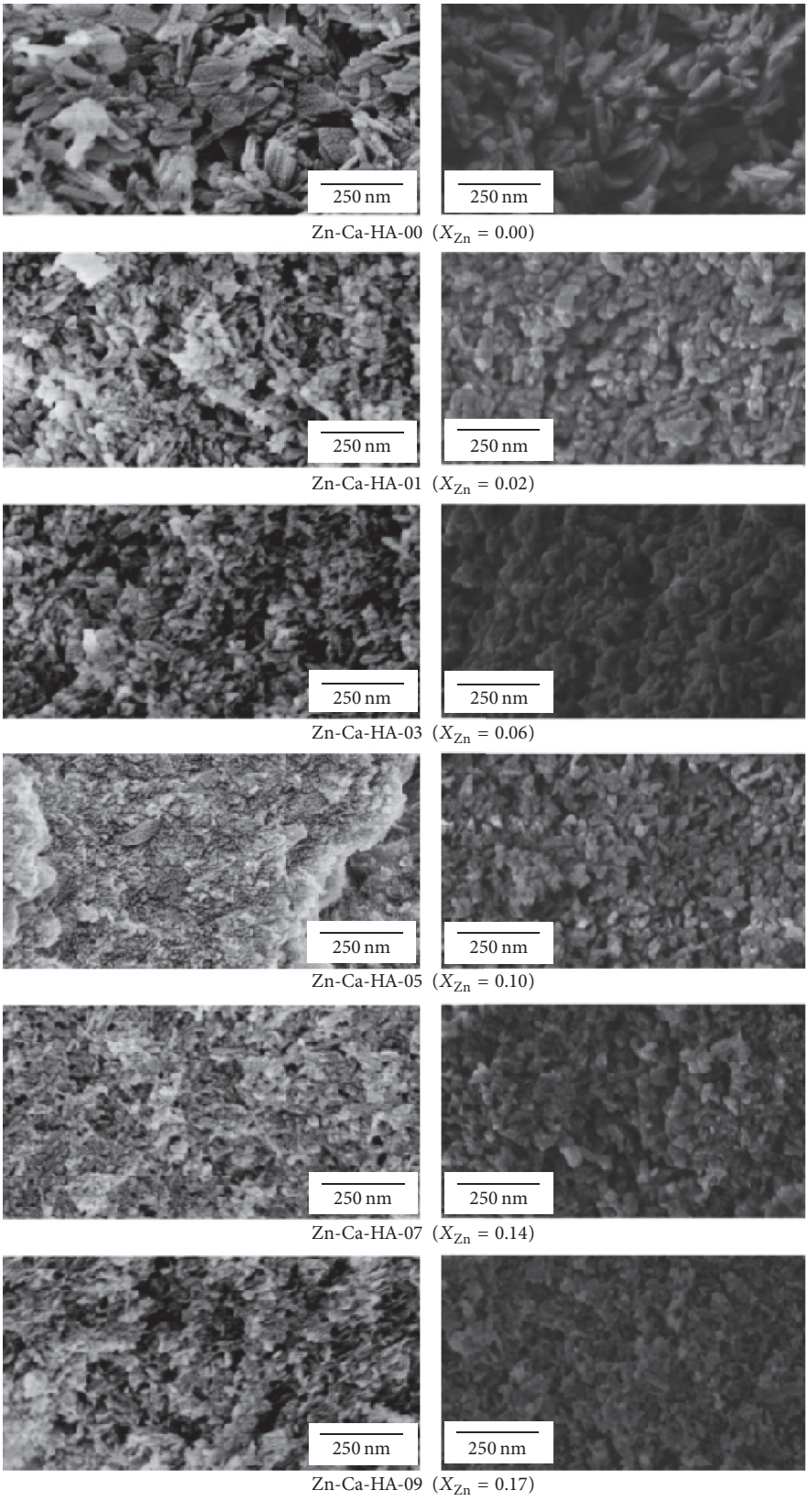

Figure 3: Field emission scanning electron micrographs (FE-SEM) of the Zn-substituted hydroxylapatites $[(Zn_xCa_{1-x})_5(PO_4)_3OH]$ before dissolution (a) and after dissolution at 25°C with an initial pH of 2.00 for 360 d (b).

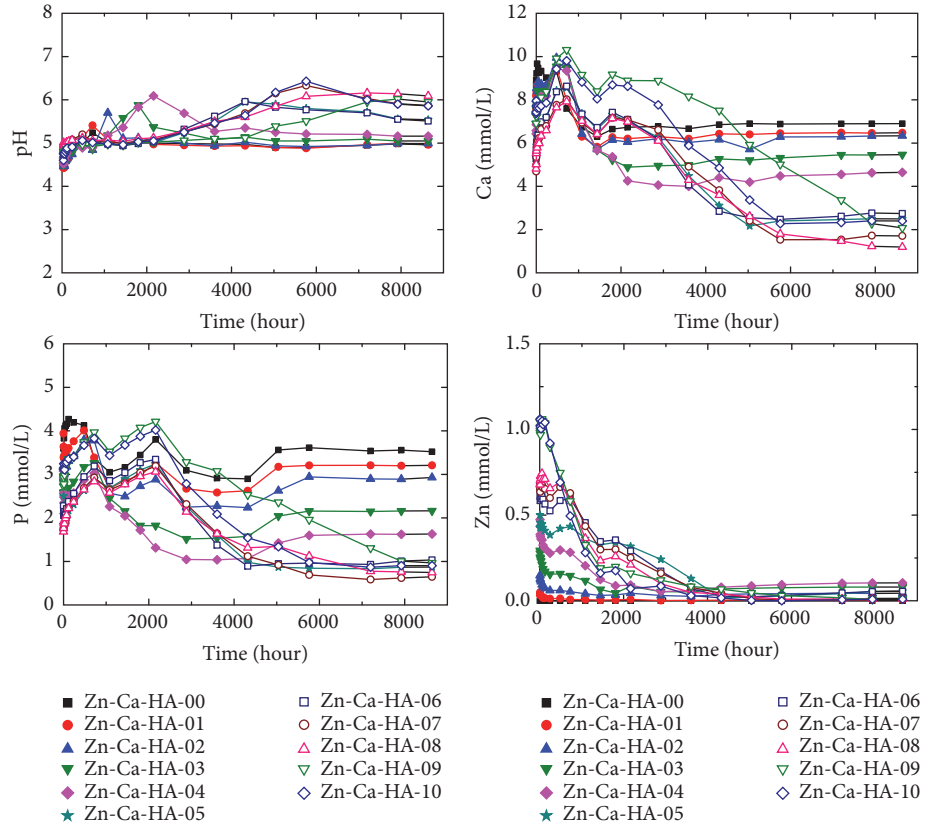

(a) pH = 2.00

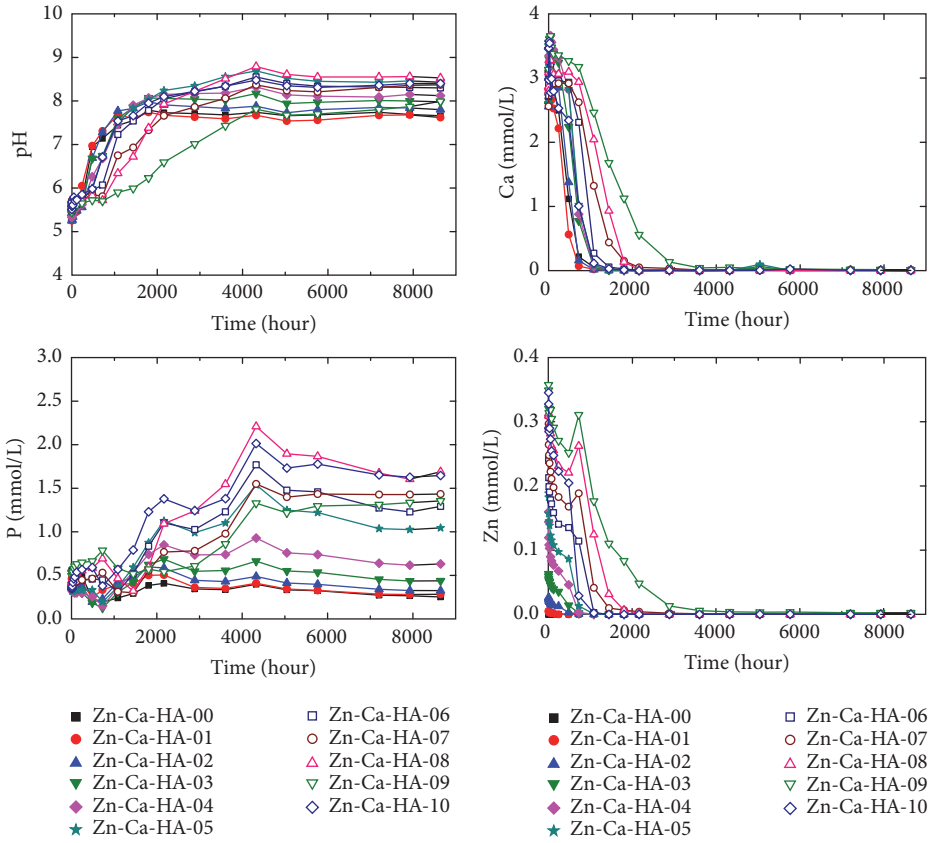

(b) pH = 5.60

Figure 4: Continued.

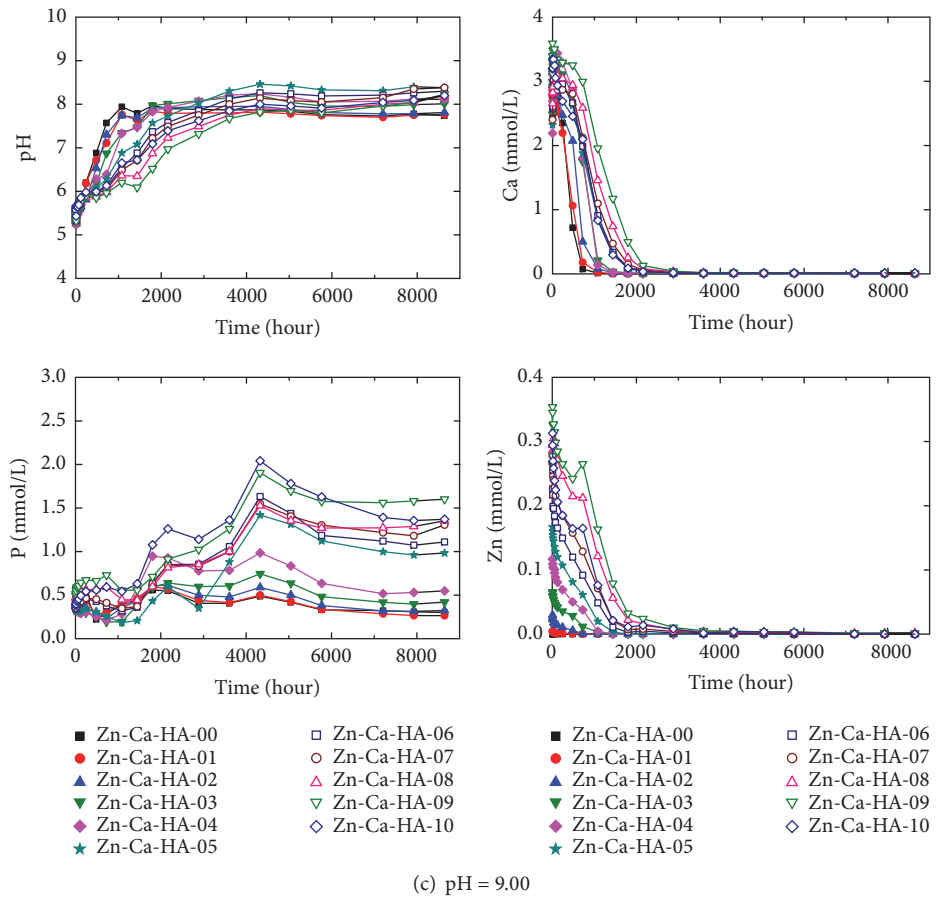

FIGURE 4: (a) Change of the solution pH and elemental concentrations with time for the dissolution of the Zn-substituted hydroxylapatites $[(Zn_xCa_{1-x})_5(PO_4)_3OH]$ at 25°C with an initial pH of 2.00 for 360 d. (b) Change of the solution pH and elemental concentrations with time for the dissolution of the Zn-substituted hydroxylapatites $[(Zn_xCa_{1-x})_5(PO_4)_3OH]$ at 25°C with an initial pH of 5.60 for 360 d. (c) Change of the solution pH and elemental concentrations with time for the dissolution of the Zn-substituted hydroxylapatites $[(Zn_xCa_{1-x})_5(PO_4)_3OH]$ at 25°C with an initial pH of 9.00 for 360 d.

Ca^{2+}, and PO_4^{3-} concentrations were greatly affected by X_{Zn} (Figure 5). The solids with lower X_{Zn} (0.00, 0.02, 0.04, 0.06, and 0.08) showed a different dissolution process from the solids with higher X_{Zn} (0.10, 0.12, 0.14, 0.16, 0.17, and 0.19) (Figures 4(a) and 5).

For the Zn-Ca apatites with lower X_{Zn} or higher X_{Ca}, the solution Ca^{2+} concentrations increased quickly with time and reached the highest values after 24~480 h dissolution. Then the concentrations decreased slowly and were stable after 1800~2160 h dissolution. The solution Zn^{2+} concentrations increased rapidly with time and reached the highest values in 1 h dissolution and then decreased progressively and attained a stable state after 4320~5040 h dissolution. For the Zn-Ca apatites with higher X_{Zn} or lower X_{Ca}, the solution Ca^{2+} concentrations increased steadily with increasing time and reached the highest values after 720 h dissolution and then decreased and became stable after 5760 h dissolution. The solution Zn^{2+} concentrations increased quickly with increasing time and achieved the highest values after 1~24 h and then decreased slowly and became stable after 4320~5040 h dissolution. The solution phosphate concentrations had an evolution trend similar to the solution Ca^{2+} concentrations. Generally, the final aqueous Ca^{2+} and phosphate concentrations decreased with the increasing X_{Zn} of the Zn-Ca apatites (Figure 5). The final aqueous Zn^{2+} concentrations increased with the increasing X_{Zn} when $X_{Zn} \leq 0.08$ and decreased with the increasing X_{Zn} when $X_{Zn} = 0.10$~0.19 (Figure 5).

For the Zn-Ca-HA dissolution at 25°C with an initial pH of 5.60 and 9.00, the solution pH, zinc, and phosphate concentrations became stable after 5040–5760 h (Figures 4(b) and 4(c)). The solution zinc and phosphate concentrations were significantly lower than those for the Zn-Ca-HA dissolution at 25°C with an initial pH of 2.00; that is, the solubility of the Zn-Ca apatites at pH 5.60 or 9.00 was considerably smaller than that at pH 2.00 (Figure 4).

The Zn-Ca apatites dissolved in the acidic solution stoichiometrically during the early stages and then nonstoichiometrically to the end of dissolution. Commonly, the solution [Zn]/[Zn + Ca] molar ratios ($X_{Zn,aq}$) decreased with increasing time and were not equal to the stoichiometric Zn/(Zn + Ca) atomic ratios of the Zn-Ca apatites (X_{Zn}) (Figure 6). During the early stage of dissolution, the solution [Zn]/[Zn + Ca]

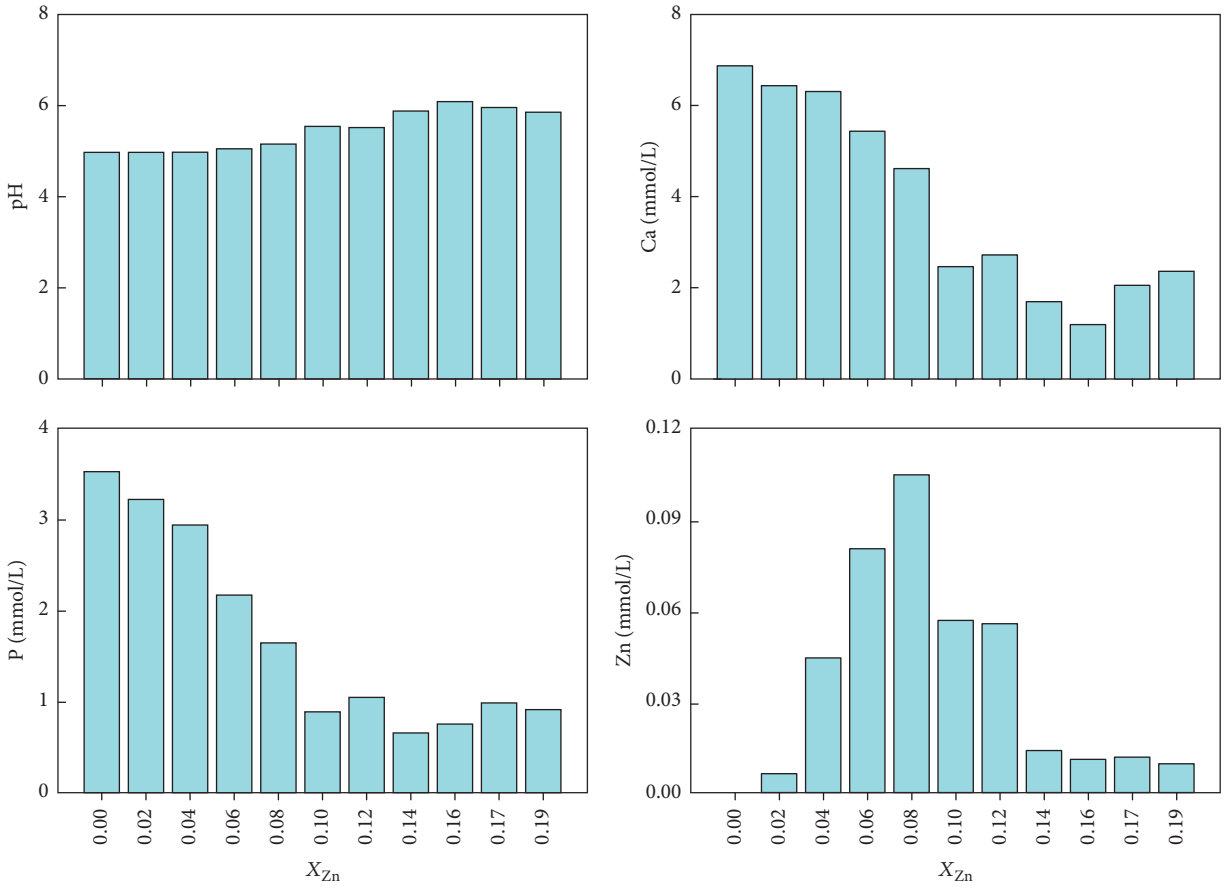

Figure 5: The solution pH and elemental concentrations after the dissolution of the Zn-substituted hydroxylapatites $[(Zn_xCa_{1-x})_5(PO_4)_3OH]$ at 25°C with an initial pH of 2.00 for 360 d.

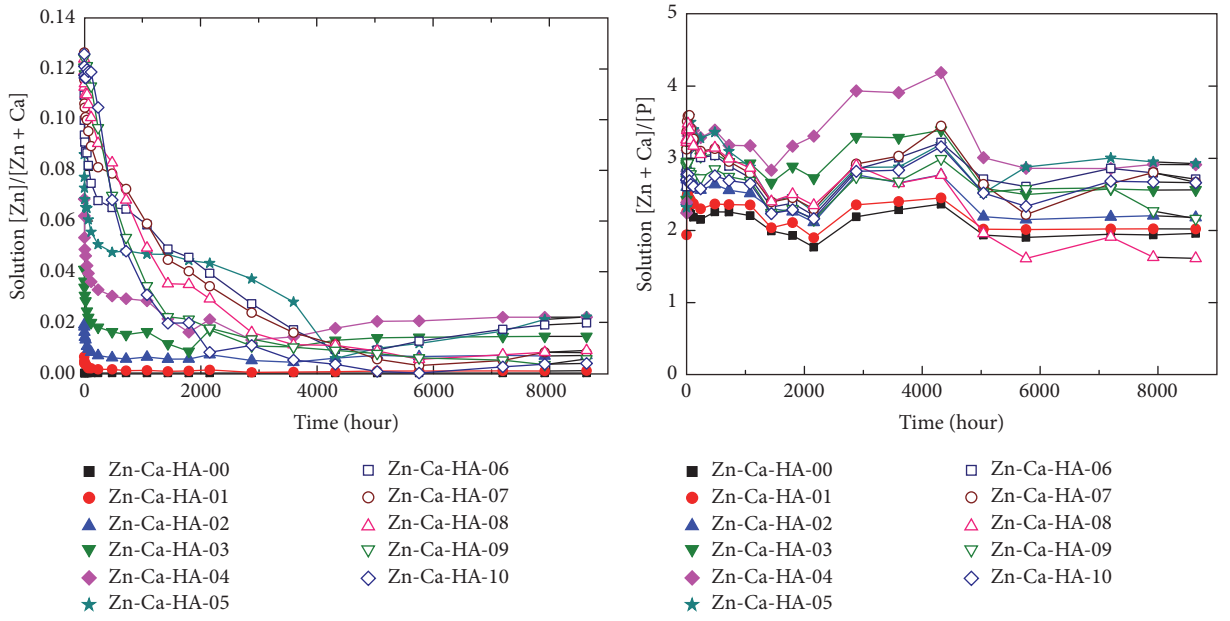

Figure 6: Change of the solution [Zn]/[Zn + Ca] and [Zn + Ca]/[P] molar ratios with time for the dissolution of the Zn-substituted hydroxylapatites $[(Zn_xCa_{1-x})_5(PO_4)_3OH]$ at 25°C.

molar ratios ($X_{Zn,aq}$) were nearly equal to the stoichiometric X_{Zn} for the Zn-Ca apatites of $X_{Zn} \leq 0.08$. The solution [Zn]/[Zn + Ca] molar ratios ($X_{Zn,aq}$) decreased steadily with time. The higher the X_{Zn}, the higher the solution [Zn]/[Zn + Ca] molar ratios ($X_{Zn,aq}$). For the dissolution of the Zn-Ca apatites with X_{Zn} = 0.10~0.19, the solution [Zn + Ca]/[P] molar ratios increased slowly with time and reached the highest values in 3~48 h; after that, the solution [Zn + Ca]/[P] molar ratios decreased steadily and became stable to the end of dissolution. For the dissolution of the Zn-Ca apatites with $X_{Zn} \leq 0.08$, the solution [Zn + Ca]/[P] molar ratios increased steadily to 2.47~3.59 after 3~48 h dissolution and reached 1.61~2.93 at the end of dissolution. The solution [Zn + Ca]/[P] molar ratios increased with the increasing X_{Zn} when $X_{Zn} \leq 0.08$ and decreased with the increasing X_{Zn} when X_{Zn} = 0.10~0.19. The solution [Ca]/[P] molar ratios changed with time in much the same manner as the solution [Zn + Ca]/[P] molar ratios because of the very low Zn concentrations in comparison to the Ca concentrations.

3.2.2. Dissolution Mechanism. For the $(Zn_xCa_{1-x})_5(PO_4)_3OH$ dissolution in acidic solution (pH 2.00 or 5.60), the H^+ consumption indicated that the adsorption of H^+ ions to the phosphate groups on the $(Zn_xCa_{1-x})_5(PO_4)_3OH$ surface could transform the phosphate groups from PO_4^{3-} to HPO_4^{2-} and enhanced the dissolution [28]. Besides, the coexisting replacement of H^+ for metallic cations on the solid surface could also cause a H^+ consumption in the $(Zn_xCa_{1-x})_5(PO_4)_3OH$ dissolution. In order to describe the H^+ depletion in the $(Zn_xCa_{1-x})_5(PO_4)_3OH$ dissolution comprehensively, many processes should be considered: the stoichiometric dissolution of $(Zn_xCa_{1-x})_5(PO_4)_3OH$ during the early stage, the substitution of $2H^+$ for Zn^{2+} or Ca^{2+} on the solid surface, and the adsorption/desorption of H^+ on the solid surface [29]. Additionally, the experimental conditions could significantly affect the apatite dissolution [30]. Various dissolution models for apatite have been proposed in literatures, but they consider only some specific dissolution aspects and cannot describe the dissolution process comprehensively [30].

Derived from the results of the present experiment and some previous works [30], the following coexisting steps or processes are considered in the $(Zn_xCa_{1-x})_5(PO_4)_3OH$ dissolution in acidic solution:

(A) Diffusion of H^+ to the solution-solid interface and adsorption of H^+ onto the Zn-Ca-HA surface.

(B) Transformation of PO_4^{3-} to HPO_4^{2-} on the Zn-Ca-HA surface in acidic solution.

(C) Desorption of Zn^{2+}, Ca^{2+}, and PO_4^{3-} ions from the Zn-Ca-HA surface and ion complexation.

(D) Readsorption of Zn^{2+}, Ca^{2+}, and/or PO_4^{3-} ions from solution back onto the Zn-Ca-HA surface.

In Steps (A) and (B), the solution pH was increased from 2.00 to 4.42~4.90 in 1 h due to the diffusion and adsorption of H^+ ions onto the Zn-Ca-HA surface for the dissolution at 25°C with an initial pH of 2.00. In Step (C), Zn^{2+}, Ca^{2+}, and PO_4^{3-} ions were removed from the Zn-Ca-HA surface to water solution. Many chemical reactions could happen in the apatite dissolution because of the structural complexity [7]. In comparison to Zn^{2+} cations, Ca^{2+} cations could be preferentially removed from the Zn-Ca-HA surface. Reaction (1) for the Zn-Ca-HA dissolution in aqueous acidic media could be significantly affected by the solution pH and together with the reactions (2)~(5) of protonation and complexation, which had caused an increase in the solution pH. As $(Zn_xCa_{1-x})_5(PO_4)_3OH$ dissolved in water, Zn^{2+} cations were transformed into $ZnOH^+$, $Zn(OH)_2^0$, $Zn(OH)_3^-$, $Zn(OH)_4^{2-}$, $ZnPO_4^-$, $ZnHPO_4$, and $ZnH_2PO_4^+$. Ca^{2+} cations were transformed into $CaOH^+$, $CaPO_4^-$, $CaHPO_4$, and $CaH_2PO_4^+$, and PO_4^{3-} cations were transformed into HPO_4^{2-}, $H_2PO_4^-$, $H_3PO_4^0$, $CaPO_4^-$, $CaHPO_4$, and $CaH_2PO_4^+$, and only a small portion of zinc, calcium, and phosphate existed in the dissociation forms such as Zn^{2+}, Ca^{2+}, and PO_4^{3-}.

$$(Zn_xCa_{1-x})_5(PO_4)_3OH = 5xZn^{2+} + (5-5x)Ca^{2+} + 3PO_4^{3-} + OH^- \quad (1)$$

$$PO_4^{3-} + nH^+ = H_nPO_4^{(3-n)-} \quad (n = 1, 2, 3) \quad (2)$$

$$Zn^{2+} + nOH^- = Zn(OH)_n^{(n-2)-} \quad (n = 1, 2, 3, 4) \quad (3)$$

$$Ca^{2+} + OH^- = Ca(OH)^+ \quad (4)$$

$$Ca^{2+} + H_nPO_4^{(3-n)-} = CaH_nPO_4^{(1-n)-} \quad (n = 0, 1, 2) \quad (5)$$

$$Zn^{2+} + H_nPO_4^{(3-n)-} = ZnH_nPO_4^{(1-n)-} \quad (n = 0, 1, 2) \quad (6)$$

In Step (D), Zn^{2+} and Ca^{2+} cations were partly readsorbed from solution onto the Zn-Ca-HA surface as an initial portion of Zn-Ca-HA dissolved and the solution Zn^{2+} and Ca^{2+} concentrations decreased as the dissolution progressed. In comparison to Ca^{2+} ions, Zn^{2+} ions were preferentially readsorbed from solution onto the Zn-Ca-HA surface, which resulted in an obvious decrease in the solution [Zn]/[Zn + Ca] molar ratios ($X_{Zn,aq}$) with time. Finally, adsorption and desorption of Zn^{2+} and Ca^{2+} reached a stable state. The solution Zn^{2+}, Ca^{2+}, and phosphate concentrations were nearly invariable from 7200 h to 8640 h for the $(Zn_xCa_{1-x})_5(PO_4)_3OH$ dissolution at 25°C with an initial pH of 2.00.

3.3. Determination of Solubility. The dissolution experiments had been carried out until the analytical uncertainty for the ion activity products calculated from the last two or three samples was less than ±0.25 log units [31]. To obtain the solubility products (K_{sp}) of the $(Zn_xCa_{1-x})_5(PO_4)_3OH$ solids, the aqueous activities of the zinc, calcium, and phosphate species for the last two or three solution samples (7200 h, 7920 h, and 8640 h) were considered in the calculation. The PHREEQC simulation results indicated that the final equilibrated solutions were unsaturated with respect to any potential secondary minerals (e.g., portlandite [$Ca(OH)_2$], lime [CaO], $CaHPO_4 \cdot 2H_2O$, $CaHPO_4$, $Ca_4H(PO_4)_3 \cdot 3H_2O$,

$Ca_3(PO_4)_2$(beta); $Zn(OH)_2$, $Zn(OH)_2$(am), and $Zn_3(PO_4)_2 \cdot 4H_2O$).

The $(Zn_xCa_{1-x})_5(PO_4)_3OH$ dissolution and the release of Zn^{2+}, Ca^{2+}, and PO_4^{3-} can be expressed using reaction (1). The equilibrium constant (K_{sp}) for reaction (1) can be expressed as follows:

$$K_{sp} = \mathrm{IAP} = \left\{Zn^{2+}\right\}^{5x} \left\{Ca^{2+}\right\}^{5-5x} \left\{PO_4^{3-}\right\}^3 \left\{OH^-\right\}, \quad (7)$$

where {} is the activity of the solution species.

The standard free energy of reaction (ΔG_r^o) can be calculated from its K_{sp} by

$$\Delta G_r^o = -5.708 \log K_{sp}. \quad (8)$$

For the dissolution reaction (1),

$$\begin{aligned} \Delta G_r^o = {} & 5x\Delta G_f^o\left[Zn^{2+}\right] + (5-5x)\,\Delta G_f^o\left[Ca^{2+}\right] \\ & + 3\Delta G_f^o\left[PO_4^{3-}\right] + \Delta G_f^o\left[OH^-\right] \\ & - \Delta G_f^o\left[(Zn_xCa_{1-x})_5(PO_4)_3OH\right] \end{aligned} \quad (9)$$

or

$$\begin{aligned} & \Delta G_f^o\left[(Zn_xCa_{1-x})_5(PO_4)_3OH\right] \\ & = 5x\Delta G_f^o\left[Zn^{2+}\right] + (5-5x)\,\Delta G_f^o\left[Ca^{2+}\right] \\ & \quad + 3\Delta G_f^o\left[PO_4^{3-}\right] + \Delta G_f^o\left[OH^-\right] - \Delta G_r^o. \end{aligned} \quad (10)$$

Table 2 lists the calculated solubility products (K_{sp}) for Ca-HA and Zn-Ca-HA, together with the solution pH, zinc, calcium, and phosphate analyses for the dissolution at 25°C with an initial pH of 2.00. By using the Gibbs free energies of formation for Zn^{2+}, Ca^{2+}, PO_4^{3-}, and OH^- from literatures [32], that is, $\Delta G_f^o[Zn^{2+}] = -147.0$ kJ/mol, $\Delta G_f^o[Ca^{2+}] = -553.54$ kJ/mol, $\Delta G_f^o[PO_4^{3-}] = -1018.8$ kJ/mol, and $\Delta G_f^o[OH^-] = -157.3$ kJ/mol, the Gibbs free energies of formation for $(Zn_xCa_{1-x})_5(PO_4)_3OH$, $\Delta G_f^o[(Zn_xCa_{1-x})_5(PO_4)_3OH]$, were also calculated (Table 2).

For calcium hydroxylapatite [$Ca_5(PO_4)_3OH$, Ca-HA], the average K_{sp} value was determined to be $10^{-57.75\pm0.12}$($10^{-57.63}$~$10^{-57.85}$) at 25°C and the Gibbs free energy of formation (ΔG_f^o) was calculated to be −6310.45 kJ/mol in the present work, which were consistent with the results of many previous researches. The K_{sp} value for $Ca_5(PO_4)_3OH$ has been reported to be $10^{-57.65}$ [14], 10^{-57} [32], $10^{-58\pm1}$ [33], 10^{-59} [34], and $10^{-58.3}$ [35].

No reports on the solubility properties of the zinc-substituted hydroxylapatites have been found in literatures. The mean K_{sp} values for $(Zn_xCa_{1-x})_5(PO_4)_3OH$ at 25°C decreased from $10^{-57.75\pm0.12}$($10^{-57.63}$~$10^{-57.85}$) to $10^{-58.60\pm0.18}$($10^{-58.42}$~$10^{-58.69}$) with the increasing X_{Zn} from 0.00 to 0.06 and then increased from $10^{-58.60\pm0.18}$ ($10^{-58.42}$–$10^{-58.69}$) to $10^{-56.63\pm0.19}$($10^{-56.44}$~$10^{-56.81}$) with the increasing X_{Zn} from 0.06 to 0.16 (Table 2 and Figure 7). This tendency was consistent with the dependency of the lattice parameter a on X_{Zn}. On the other hand, the corresponding free energies of formation (ΔG_f^o) increased lineally ($R^2 = 0.9997$) from −6310.45 kJ/mol to −5979.39 kJ/mol with the increasing X_{Zn} from 0.00 to 0.16 (Table 2 and Figure 7).

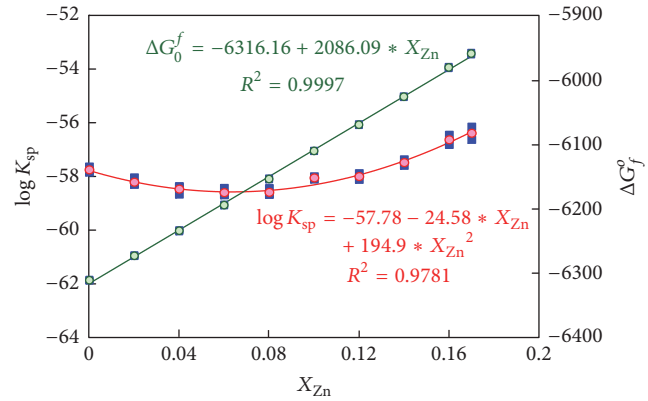

Figure 7: Change of the solubility product and the free energy of formation with the increasing X_{Zn} for the Zn-substituted hydroxylapatites [$(Zn_xCa_{1-x})_5(PO_4)_3OH$] at 25°C.

4. Summary

Examination by using XRD and FE-SEM confirmed that no obvious variation of the Zn-Ca apatites was observed in the dissolution. The cell parameter a of the Zn-Ca apatites decreased with the increasing X_{Zn} from 0.00 to 0.08, increased with the increasing X_{Zn} from 0.08 to 0.12, and then decreased with the increasing X_{Zn} from 0.12 to 0.16. When $X_{Zn} > 0.16$, ammonium zinc phosphate (NH_4ZnPO_4) was also observed in the precipitates. No apatite phase formed when the [Zn]/[Zn + Ca] molar ratio in the mixed aqueous solution was greater than 0.20.

The solution concentrations of zinc, calcium, and phosphate were greatly correlated to the Zn/(Zn + Ca) molar ratios of the Zn-Ca apatites (X_{Zn}). For the dissolution at 25°C with an initial pH of 2.00, the solids of $X_{Zn} \leq 0.08$ showed a different dissolution process from the solids of $X_{Zn} = 0.10$~0.16. The final solution pH values increased, and the final solution Ca^{2+} and phosphate concentrations decreased with the increasing X_{Zn}. The final solution Zn^{2+} concentrations increased with the increasing X_{Zn} when $X_{Zn} \leq 0.08$ and decreased with the increasing X_{Zn} when $X_{Zn} = 0.08$~0.16. For the dissolution at 25°C with an initial pH of 5.60 and 9.00, the solution zinc and phosphate concentrations were significantly lower than those for the dissolution at 25°C with an initial pH of 2.00. Generally, the solution [Zn]/[Zn + Ca] molar ratios ($X_{Zn,aq}$) were lower than the X_{Zn} values of the corresponding solids. Ca^{2+} ions were preferentially removed from solid to solution in comparison to Zn^{2+} ions, while Zn^{2+} ions were preferentially readsorbed from solution onto the Zn-Ca-HA surface, which resulted in a significant decrease of the solution [Zn]/[Zn + Ca] molar ratios ($X_{Zn,aq}$) with time.

The $(Zn_xCa_{1-x})_5(PO_4)_3OH$ dissolution is considered to include four coexisting steps: diffusion and adsorption of H^+

Table 2: Analytical data and solubility determination of the Zn-substituted hydroxylapatites (25°C and initial pH 2.00).

Sample	Dissolution time (h)	pH	Concentration (mmol/L)			$\log K_{sp}$	Average $\log K_{sp}$	ΔG_f^o (kJ/mol)	Average ΔG_f^o (kJ/mol)
			Zn	Ca	P				
$(Zn_{0.00}Ca_{1.00})_5(PO_4)_3OH$	7200	4.95	0.0000	6.8916	3.5385	−57.85	−57.75	−6311.58	−6311.03
	7920	4.98	0.0000	6.8941	3.5578	−57.63		−6310.34	
	8640	4.96	0.0000	6.9015	3.5207	−57.77		−6311.17	
$(Zn_{0.02}Ca_{0.98})_5(PO_4)_3OH$	7200	4.96	0.0055	6.4824	3.2091	−58.30	−58.21	−6273.53	−6273.00
	7920	5.00	0.0052	6.4624	3.1978	−58.03		−6271.98	
	8640	4.96	0.0061	6.4774	3.2075	−58.29		−6273.48	
$(Zn_{0.04}Ca_{0.96})_5(PO_4)_3OH$	7200	4.95	0.0442	6.2927	2.8960	−58.67	−58.47	−6234.97	−6233.84
	7920	4.99	0.0428	6.3302	2.8905	−58.38		−6233.33	
	8640	4.99	0.0443	6.3376	2.9283	−58.36		−6233.21	
$(Zn_{0.06}Ca_{0.94})_5(PO_4)_3OH$	7200	5.09	0.0797	5.4544	2.1479	−58.42	−58.60	−6192.92	−6193.93
	7920	5.05	0.0800	5.4494	2.1599	−58.69		−6194.45	
	8640	5.05	0.0803	5.4643	2.1631	−58.68		−6194.41	
$(Zn_{0.08}Ca_{0.92})_5(PO_4)_3OH$	7200	5.20	0.1025	4.5511	1.6278	−58.43	−58.59	−6152.30	−6153.22
	7920	5.16	0.1043	4.6260	1.6223	−58.68		−6153.72	
	8640	5.16	0.1048	4.6434	1.6304	−58.66		−6153.63	
$(Zn_{0.10}Ca_{0.90})_5(PO_4)_3OH$	7920	5.56	0.0541	2.5026	0.8662	−57.99	−58.05	−6109.13	−6109.47
	8640	5.54	0.0566	2.4951	0.8717	−58.11		−6109.81	
$(Zn_{0.12}Ca_{0.88})_5(PO_4)_3OH$	7920	5.55	0.0536	2.7671	1.0083	−57.88	−58.00	−6067.83	−6068.52
	8640	5.51	0.0554	2.7446	1.0331	−58.12		−6069.22	
$(Zn_{0.14}Ca_{0.86})_5(PO_4)_3OH$	7920	5.91	0.0142	1.7239	0.6199	−57.36	−57.48	−6024.22	−6024.89
	8640	5.87	0.0138	1.7079	0.6457	−57.59		−6025.57	
$(Zn_{0.16}Ca_{0.84})_5(PO_4)_3OH$	7920	6.14	0.0101	1.2296	0.7606	−56.44	−56.63	−5978.31	−5979.39
	8640	6.09	0.0108	1.1927	0.7458	−56.81		−5980.46	
$(Zn_{0.17}Ca_{0.83})_5(PO_4)_3OH$	7920	6.02	0.0076	2.2766	1.0067	−56.14	−56.38	−5956.27	−5957.67
	8640	5.95	0.0117	2.0809	0.9673	−56.63		−5959.06	
$(Zn_{0.19}Ca_{0.81})_5(PO_4)_3OH$	7920	5.90	0.0084	2.4043	0.9030	−45.85	−45.96	−5856.88	−5857.53
	8640	5.86	0.0092	2.3978	0.9040	−46.08		−5858.19	

onto the solid surface, transformation of PO_4^{3-} to HPO_4^{2-} on the solid surface, desorption and ion complexation of Zn^{2+}, Ca^{2+}, and PO_4^{3-}, and readsorption of these ions from solution back onto the solid surface.

The mean K_{sp} values for $(Zn_xCa_{1-x})_5(PO_4)_3OH$ at 25°C decreased from $10^{-57.75}$ to $10^{-58.59}$ with the increasing X_{Zn} from 0.00 to 0.08 and then increased from $10^{-58.59}$ to $10^{-56.63}$ with the increasing X_{Zn} from 0.08 to 0.16. This tendency was consistent with the dependency of the lattice parameter a on X_{Zn}. The corresponding free energies of formation (ΔG_f^o) increased lineally from −6310.45 kJ/mol to −5979.39 kJ/mol with the increasing X_{Zn} from 0.00 to 0.16.

Conflicts of Interest

The authors declare that there are no conflicts of interest regarding the publication of this paper.

Acknowledgments

The authors thank the Guangxi Collaborative Innovation Centre for Water Pollution Control and Water Safety in Karst Area for the research assistance and the financial supports from the National Natural Science Foundation of China (51638006, 41263009), the Guangxi Science and Technology Development Project (GuiKeGong14124004-3-3), and the Provincial Natural Science Foundation of Guangxi (2014GXNSFBA118054, 2012GXNSFDA053022).

References

[1] A. V. Knyazev, E. N. Bulanov, and V. Z. Korokin, "Thermal expansion of solid solutions in apatite binary systems," *Materials Research Bulletin*, vol. 61, pp. 47–53, 2015.

[2] J. R. Guerra-López, G. A. Echeverría, J. A. Güida, R. Viña, and G. Punte, "Synthetic hydroxyapatites doped with Zn(II) studied

by X-ray diffraction, infrared, Raman and thermal analysis," *Journal of Physics and Chemistry of Solids*, vol. 81, pp. 57–65, 2015.

[3] T. G. Peñaflor Galindo, T. Kataoka, S. Fujii, M. Okuda, and M. Tagaya, "Preparation of nanocrystalline zinc-substituted hydroxyapatite films and their biological properties," *Colloids and Interface Science Communications*, vol. 10-11, pp. 15–19, 2016.

[4] A. Giera, M. Manecki, T. Bajda, J. Rakovan, M. Kwaśniak-Kominek, and T. Marchlewski, "Arsenate substitution in lead hydroxyl apatites: A Raman spectroscopic study," *Spectrochimica Acta - Part A: Molecular and Biomolecular Spectroscopy*, vol. 152, pp. 370–377, 2016.

[5] C. Drouet, "A comprehensive guide to experimental and predicted thermodynamic properties of phosphate apatite minerals in view of applicative purposes," *Journal of Chemical Thermodynamics*, vol. 81, pp. 143–159, 2015.

[6] E. S. Thian, T. Konishi, Y. Kawanobe et al., "Zinc-substituted hydroxyapatite: a biomaterial with enhanced bioactivity and antibacterial properties," *Journal of Materials Science: Materials in Medicine*, vol. 24, no. 2, pp. 437–445, 2013.

[7] Å. Bengtsson, A. Shchukarev, P. Persson, and S. Sjöberg, "A solubility and surface complexation study of a non-stoichiometric hydroxyapatite," *Geochimica et Cosmochimica Acta*, vol. 73, no. 2, pp. 257–267, 2009.

[8] F. Ren, R. Xin, X. Ge, and Y. Leng, "Characterization and structural analysis of zinc-substituted hydroxyapatites," *Acta Biomaterialia*, vol. 5, no. 8, pp. 3141–3149, 2009.

[9] Y. Tang, H. F. Chappell, M. T. Dove, R. J. Reeder, and Y. J. Lee, "Zinc incorporation into hydroxylapatite," *Biomaterials*, vol. 30, no. 15, pp. 2864–2872, 2009.

[10] M. Li, X. Xiao, R. Liu, C. Chen, and L. Huang, "Structural characterization of zinc-substituted hydroxyapatite prepared by hydrothermal method," *Journal of Materials Science: Materials in Medicine*, vol. 19, no. 2, pp. 797–803, 2008.

[11] I. Mayer and J. D. B. Featherstone, "Dissolution studies of Zn-containing carbonated hydroxyapatites," *Journal of Crystal Growth*, vol. 219, no. 1-2, pp. 98–101, 2000.

[12] H. Esfahani, E. Salahi, A. Tayebifard, M. Rahimipour, and M. Keyanpour-Rad, "Influence of zinc incorporation on microstructure of hydroxyapatite to characterize the effect of pH and calcination temperatures," *Journal of Asian Ceramic Societies*, vol. 2, no. 3, pp. 248–252, 2014.

[13] K. P. Tank, K. S. Chudasama, V. S. Thaker, and M. J. Joshi, "Pure and zinc doped nano-hydroxyapatite: synthesis, characterization, antimicrobial and hemolytic studies," *Journal of Crystal Growth*, vol. 401, pp. 474–479, 2014.

[14] Y. Zhu, Z. Zhu, X. Zhao, Y. Liang, L. Dai, and Y. Huang, "Characterization, dissolution and solubility of cadmium-calcium hydroxyapatite solid solutions at 25°C," *Chemical Geology*, vol. 423, pp. 34–48, 2016.

[15] G. Qian, X. Xu, W. Sun, Y. Xu, and Q. Liu, "Preparation, characterization, and stability of calcium zinc hydrophosphate," *Materials Research Bulletin*, vol. 43, no. 12, pp. 3463–3473, 2008.

[16] K. Skartsila and N. Spanos, "Surface characterization of hydroxyapatite: potentiometric titrations coupled with solubility measurements," *Journal of Colloid and Interface Science*, vol. 308, no. 2, pp. 405–412, 2007.

[17] N. Harouiya, C. Chaïrat, S. J. Köhler, R. Gout, and E. H. Oelkers, "The dissolution kinetics and apparent solubility of natural apatite in closed reactors at temperatures from 5 to 50°C and pH from 1 to 6," *Chemical Geology*, vol. 244, no. 3-4, pp. 554–568, 2007.

[18] J. Gómez del Río, P. Sanchez, P. J. Morando, and D. S. Cicerone, "Retention of Cd, Zn and Co on hydroxyapatite filters," *Chemosphere*, vol. 64, no. 6, pp. 1015–1020, 2006.

[19] M. Kwaśniak-Kominek, J. Matusik, T. Bajda et al., "Fourier transform infrared spectroscopic study of hydroxylpyromorphite $Pb_{10}(PO_4)_6OH_2$—hydroxylmimetite $Pb_{10}(AsO_4)_6(OH)_2$ solid solution series," *Polyhedron*, vol. 99, pp. 103–111, 2015.

[20] K. Zhu, K. Yanagisawa, R. Shimanouchi, A. Onda, and K. Kajiyoshi, "Preferential occupancy of metal ions in the hydroxyapatite solid solutions synthesized by hydrothermal method," *Journal of the European Ceramic Society*, vol. 26, no. 4-5, pp. 509–513, 2006.

[21] C. Ergun, T. J. Webster, R. Bizios, and R. H. Doremus, "Hydroxylapatite with substituted magnesium, zinc, cadmium, and yttrium. I. Structure and microstructure," *Journal of Biomedical Materials Research*, vol. 59, no. 2, pp. 305–311, 2002.

[22] T. J. Webster, C. Ergun, R. H. Doremus, and R. Bizios, "Hydroxylapatite with substituted magnesium, zinc, cadmium, and yttrium. II. Mechanisms of osteoblast adhesion," *Journal of Biomedical Materials Research*, vol. 59, no. 2, pp. 312–317, 2002.

[23] D. L. Parkhurst and C. A. J. Appelo, "Description of input and examples for PHREEQC version 3—a computer program for speciation, batch-reaction, one-dimensional transport, and inverse geochemical calculations," in *U.S. Geological Survey Techniques and Methods, Book 6*, chapter A43, pp. 1–497, 2013.

[24] J. D. Allison, D. S. Brown, and K. J. Novo-Gradac, *MINTEQA2/PRODEFA2, A Geochemical Assessment Model for Environmental Systems: Version 3.0 User's Manual*, EPA/600/3-91/021, Environmental Research Laboratory, Office of Research and Development, U.S. Environmental Protection Agency, 1991.

[25] F. Miyaji, Y. Kono, and Y. Suyama, "Formation and structure of zinc-substituted calcium hydroxyapatite," *Materials Research Bulletin*, vol. 40, no. 2, pp. 209–220, 2005.

[26] A. J. Andara, D. M. Heasman, Á. Fernández-González, and M. Prieto, "Characterization and crystallization of $Ba(SO_4,SeO_4)$ solid solution," *Crystal Growth and Design*, vol. 5, no. 4, pp. 1371–1378, 2005.

[27] R. Z. LeGeros, C. B. Bleiwas, M. Retino, R. Rohanizadeh, and J. P. LeGeros, "Zinc effect on the in vitro formation of calcium phosphates: relevance to clinical inhibition of calculus formation," *American Journal of Dentistry*, vol. 12, no. 2, pp. 65–71, 1999.

[28] J. Christoffersen, M. R. Christoffersen, and T. Johansen, "Some new aspects of surface nucleation applied to the growth and dissolution of fluorapatite and hydroxyapatite," *Journal of Crystal Growth*, vol. 163, no. 3, pp. 304–310, 1996.

[29] C. Chaïrat, E. H. Oelkers, J. Schott, and J.-E. Lartigue, "Fluorapatite surface composition in aqueous solution deduced from potentiometric, electrokinetic, and solubility measurements, and spectroscopic observations," *Geochimica et Cosmochimica Acta*, vol. 71, no. 24, pp. 5888–5900, 2007.

[30] S. V. Dorozhkin, "A review on the dissolution models of calcium apatites," *Progress in Crystal Growth and Characterization of Materials*, vol. 44, no. 1, pp. 45–61, 2002.

[31] D. Baron and C. D. Palmer, "Solid-solution aqueous-solution reactions between jarosite (KFe3(SO4)2(OH)6) and its chromate analog," *Geochimica et Cosmochimica Acta*, vol. 66, no. 16, pp. 2841–2853, 2002.

[32] W. Stumm and J. J. Morgan, *Aquatic Chemistry, Chemical Equilibria and Rates in Natural Waters*, John Wiley & Sons, New York, NY, USA, 1996.

[33] E. Valsami-Jones, K. V. Rggnarsdottir, A. Putnis, D. Bosbach, A. J. Kemp, and G. Cressey, "The dissolution of apatite in the presence of aqueous metal cations at pH 2-7," *Chemical Geology*, vol. 151, no. 1-4, pp. 215–233, 1998.

[34] W. E. Brown, T. M. Gregory, and L. C. Chow, "Effects of fluoride on enamel solubility and cariostasis," *Caries Research*, vol. 11, supplement 1, pp. 118–141, 1977.

[35] H. McDowell, T. M. Gregory, and W. E. Brown, "Solubility of $Ca_5(P0_4)_3OH$ in the system $Ca(OH)_2$-H_3P0_4-H_20 at 5, 15, 25, and 37°C," *Journal of Research of the National Bureau of Standards—A. Physics and Chemistry*, vol. 81A, no. 2-3, pp. 273–281, 1977.